Genome structure and evolution of *Antirrhnum majus* L.

Miaomiao Li[1,7*], Dongfen Zhang[1*], Hui Zhang[1,7*], Qiang Gao [3*], Bin Ma [3*] , Chunhai Chen[2*], Yingfeng Luo[6], Yinghao Cao[3], Qun Li[1], Yu'e Zhang[1], Han Guo[1,7], Junhui Li[1,7], Yanzhai Song[1,7], Yue Zhang[1,7], Lucy Copsey[4], Annabel Whibley[4], Yan Li[3], Ming qi[3], Jiawei Wang[5], Yan Chen[2], Dan Wang[2], Jinyang Zhao[2], Guocheng Liu[2], Bin Wu[2], Lili Yu[2], Chunyan Xu[2], Jiang Li[2], Shancen Zhao[2], Yijing Zhang[5], Songnian Hu[6], Chengzhi Liang[a,3], Ye Yin[a,2], Enrico Coen[a,4], Yongbiao Xue[a,1,6,7]

[1]State Key Laboratory of Plant Cell and Chromosome Engineering and National Center of Plant Gene Research, Institute of Genetics and Developmental Biology, Chinese Academy of Sciences, Beijing 100101, China

[2]BGI-Shenzhen, Main Building, Beishan Industrial Zone, Yantian District, Shenzhen, 518083, China

[3]State Key Laboratory of Plant Genomics, Institute of Genetics and Developmental Biology, Chinese Academy of Sciences, Beijing 100101, China

[4]John Innes Centre, Norwich, NR4 7UH, United Kingdom

[5]National Laboratory of Plant Molecular Genetics, CAS Center for Excellence in Molecular Plant Sciences, Institute of Plant Physiology and Ecology, Shanghai Institutes for Biological Sciences, Chinese Academy of Sciences, 300 Fenglin Road, Shanghai 200032, China

[6]Beijing Institute of Genomics, Chinese Academy of Sciences, Beijing 100101, China

[7]University of Chinese Academy of Sciences, Beijing 100190, China

[*]These authors contributed equally to this work.

[a]Correspondence authors:

Yongbiao Xue

Institute of Genetics and Developmental Biology, Chinese Academy of Sciences, 1 West Beichen Road, Chaoyang District, Beijing 100101, China

Tel: 86-10-64801181

Fax: 86-10-64801292

E-mail: ybxue@genetics.ac.cn

Enrico Coen

John Innes Centre, Norwich, NR4 7UH, United Kingdom

Email: enrico.coen@jic.ac.uk

Ye Yin

BGI-Shenzhen, Main Building, Beishan Industrial Zone, Yantian District, Shenzhen, 518083, China

Email: yinye@genomics.cn

Chengzhi Liang

Institute of Genetics and Developmental Biology, Chinese Academy of Sciences, 1 West Beichen Road, Chaoyang District, Beijing 100101, China

Email: cliang@genetics.ac.cn

Abstract

Snapdragon (*Antirrhinum majus* L.), a member of Plantaginaceae, is an important model for plant genetics and molecular studies on plant growth and development, transposon biology and self-incompatibility. Here we report a high-quality genome assembly of *A. majus* cultivated JI7 (*A. majus* cv.JI7) of a 510 Mb with 37,714 annotated protein-coding genes. The scaffolds covering 97.12% of the assembled genome were anchored on 8 chromosomes. Comparative and evolutionary analyses revealed that Plantaginaceae and Solanaceae diverged from their most recent ancestor around 62 million years ago (MYA). We also revealed the genetic architectures associated with complex traits such as flower asymmetry and self-incompatibility

including a unique TCP duplication around 46-49 MYA and a near complete *ψS*-locus of ca.2 Mb. The genome sequence obtained in this study not only provides the first genome sequenced from Plantaginaceae but also bring the popular plant model system of *Antirrhinum* into a genomic age.

Introduction

The genus *Antirrhinum* belongs to the Plantaginaceae family and includes about 20 species with the chromosome number of 2n=16[1]. The cultivated *A. majus* was domesticated as an ornamental in garden over two thousand years ago. *Antirrhinum* originated in Europe and are mainly distributed in Europe, Asia, and Africa around the Mediterranean coast. Different species in *Antirrhinum* have obvious differentiation in flower color, fragrance, flower pattern and flowering time; and interspecific hybridization often occurred among them. The genus has evolved two major mating systems, insect pollination (entomophily) and self-incompatibility (SI), to promote out-cross[1,2,3].

Antirrhinum has served as an excellent system in molecular genetics and developmental biology studies in the past three decades because of its active transposable elements for generating rich mutant resources[4]. Several key genes were first cloned in *Antirrhinum* including the founding members of MADS (*DEFICIENS*) and TCP (*CYCLOIDEA*) gene families, a MYB gene *MIXTA* controlling petal epidermis formation, three MYB transcription factors encoded by *ROSEAL*, *ROSEAL2* and *VENOSA* controlling flower color intensity and the *SLF*s (***S*-*L***ocus ***F***-box) controlling self-incompatibility[5-13]. Most of these genes were identified by a representative “cut and paste” transposon-tagging systems in *Antirrhinum* involved in flower development, floral-organ identity and inflorescence architecture [1,14].

However, it remains unclear what constitutes their genomic architectures and how they evolve without the genome structure of the regions containing these genes. Here, we report a high-quality genome sequence of *A. majus* of 510 Mb assembled with 37,714 annotated protein-coding genes combining using whole-genome shotgun sequencing of Illumina short reads and single-molecule, real time (SMRT) sequencing long reads from Pacific Biosciences (PacBio) platform. Most of the assembled sequences were anchored to chromosomes to form 8 pseudomolecules using a genetic map. Furthermore, comparative genomic analysis revealed that *Antirrhinum* was derived from related families about 62 MYA and a whole genome duplication event occurred around 46-49 MYA. We also showed a near complete genomic structure of the pseudo (ψ) *S*-locus of *A. majus* of ca. 2 Mb, which consists of 102 genes from *RAD* to *SLF37* genes[15]. The genome sequence provided in this study will accelerate genomic and evolutionary studies on this classical model species.

Results

Genome sequencing, assembly and annotation of *A. majus*

We sequenced a highly inbred *Antirrhinum* line (*A. majus* cv. JI7 with eight linkage groups) using the combination Illumina short read and Pacific Biosciences (PacBio) long read sequencing technologies by the genotyping-by-sequencing (GBS) method[16]. The genome size was estimated to be about 520 M based on kmer distribution. We used Canu to correct and assemble PacBio reads into contigs and using SSPACE for scaffolding with Mate-paired short reads. The assembled genome size was 510 Mb with a contig and scaffold N50 sizes of 733 kb and 3,742 kb, respectively (Figure 1, Table 1, Supplementary Figure1 and Supplementary Table 1-2). To anchor *Antirrhinum* genome sequence to chromosomes, we used JoinMap 4.1 to designed marks from re-sequencing 48 recombinant inbred lines (RIL) that derived from *A. majus* crossed to the self-incompatible species *A. charidemi*. Eight linkage groups covered 496.9Mb, representing 97.12% of the assembled *Antirrhinum* genome. The

largest chromosome 2 was estimated ca. 75.4 Mb, whereas the smallest chromosome 4 ca. 50.9 Mb and chromosome 8 ca. 57.0 Mb. The average ratio of physical to genetic distance was estimated to be 753.6 kb/cM. The rate of genetic and physical distance showed lower recombination rate at the pericentromeric regions of chr4, chr6, chr7 and chr8, together with the locations of their centromeres. Validations by known genetic markers and FISH (fluorescence *in situ* hybridization) showed that the linkage groups represent a high-quality physical map (Supplementary Figure 2-4 and Supplementary Table 3).

To validate genome quality and integrity, the completeness of the assembled euchromatic portion was examined by comparing 25,651 public ESTs of *Antirrhinum* from NCBI (http://www.ncbi.nlm.nih.gov/nucest/?term=EST%20*Antirrhinum*) and 96.59% EST sequences were mapped on the assembled genome. Next, we did the alignments between three Bacterial Artificial Chromosome (BAC) sequences and the assembled *Antirrhinum* genome, indicating an average 98.3% of euchromatin coverage. We also used BUSCO analysis to compare the quality of the assembled *Antirrhinum* genome sequence to that of other published plant genomes and showed a high quality of the assembled sequence data (Supplementary Figure 5-7).

We predicted a total of 37,714 protein-coding genes with an average transcript length of 3,166 bp by using *Antirrhinum* EST sequences and RNA-seq data from six major tissues: leaf, root, stem, stamen, pistil and pollen (http://bioinfo.sibs.ac.cn/Am/, Supplementary Excel 1). Approximately 89.11% of all genes could be functionally annotated. The average gene density in *Antirrhinum* is one gene per 15.5 kb, which is about three times lower than Arabidopsis (one gene/4.5 kb) and slightly higher than tomato (one gene/25.7 kb). Genes are also distributed unevenly, being more abundant in the ends of chromosomal arms. We also identified 981 transfer RNA, 800 microRNA, 10 ribosomal RNA and 622 small nuclear RNA families. A total of 268.3 Mb (43.8%) sequences were annotated as repeats including a wealth of class I

(Retrotransposon: 182.8 Mb), class II (DNA transposon: 41.1 Mb) elements, accounting for 52.6% of the assembled genome (Supplementary Table 4-7).

To detect the intragenomic organization in *A. majus*, self-alignment analysis was employed to reveal the duplicated and triplication regions between and within chromosomes. A whole genome triplication occurred between chromosome 1, 7 and 8, between chromosome 4, 6 and 8. Paralogous relationships among eight *Antirrhinum* chromosomes revealed 45 major duplications and 2 triplications by dot plot analyses. Collectively, forty-seven major intra-syntenic blocks spanning 1,841 pairs of paralogous genes were identified on the eight chromosomes (Figure 1, Supplementary Excel 2).

Taken together, the *Antirrhinum* genome generated in this study represents a high-quality chrome-scale genome map.

Comparative genomics and evolution of *A. majus*

To compare *Antirrhinum* genome with other plant genomes, we first examined the synteny of *Antirrhinum* chromosomes. The results showed that homologous genes in *Antirrhinum* chromosomes 1, 4, 5, 6, 7 and 8 are collinear to tomato chromosome 6/7/11, 3/8, 1/4/5, 2/3, 12 and 9, respectively, indicating that these chromosomes shared similar evolutionary histories (Figure 2a). Base on the collinearity of gene pairs, we calculated the density distribution of synonymous substitution rate per gene (*Ks*) between collinear paralogous genes and inferred the time of whole-genome duplication (WGD) events in *Antirrhinum.* A peak at around 0.57-0.60 showed a recent WGD in *Antirrhinum* occurred around 46-49 Mya corresponding to a β event [17] (Figure 2b). We then compared the complexity of gene families between *Antirrhinum* and other species and showed that 9,503 gene families are shared by *Antirrhinum*, *Arabidopsis*, rice, and tomato. 6,677 genes families were possibly contracted in

158 *Antirrhinum* while the other 3,778 gene families expanded including the F-box protein
159 family being expanded significantly (Figure 2c).

160 To examine the *Antirrhinum* genome evolution, we performed all-against-all
161 comparison analyses for the evolution of gene families and constructed a phylogenetic
162 tree of nine angiosperm species (*A. majus*, *A. thaliana*, *A. trichopoda*, *C. papaya*, *O.*
163 *sativa*, *P. hybrida*, *P. mume*, *S.lycopersicum*, *S. tuberosum*and *V. vitis*) based on the
164 shared 2114 single-copy genes of *Antirrhinum*. The divergence times of *C. papaya*-*A.*
165 *thaliana* (55.1~90.6 million years ago) and dicot-monocot (123.9~228.5 million years
166 ago) were used for calibration derived from the published data (Figure 2d). Taken
167 together, these results showed that *Antirrhinum* lineage was split from potato and
168 tomato lineages around 97 MYA with its own recent WGD event occurred about
169 46-49 MYA.

170

171 **Evolution of floral asymmetry and TCP family**

172 *A. majus* has served as the genetic model of floral symmetry. Recent studies have
173 revealed the floral asymmetry in *A. majus* is largely controlled by two TCP family
174 TFs (CYC and DICH) [7,8,18]. To explore their evolution, we compared the composition
175 and number of TCP family in several sequenced angiosperms with floral symmetry
176 information. Both eudicot and monocot share a CYC/DICH embedded CYC/TB1
177 clade, while radial flower basal angiosperm *A. trichopoda* lacks any members of class
178 II CYC/TB1 clade, suggesting that class I and class II CIN clade were more ancient
179 than class II CYC/TB1 clade, and the initial role for CYC/TB1 clade was not likely
180 involved in floral symmetry control (Figure 3 and Supplementary Excel 3).

181 We identified a total of 30 putative functional TCP family genes, including 13
182 class I genes, 10 class II CIN clade genes and 7 class II CYC/TB1 clade genes.
183 Syntenic block and *Ks* analyses of the orthologous gene pairs revealed that the recent
184 whole genome duplication and tandem duplication contributed to the expansion of

TCP family members, especially for the *CYC*/*DICH* embedded CYC/TB1 clade (Figure 3 and Supplementary Table 8). Previous studies indicated *CYC* and *DICH* have overlapping expression patterns in floral meristems in *A. majus* and the fully radial flower only appeared in *CYC*/*DICH* double mutants, suggesting the genetic robustness of zygomorphic flower control. To estimate the time of *CYC* and *DICH* duplication event, we performed *Ks* analysis of the syntenic block embedding *CYC*/*DICH* with 79 homologous gene pairs (Supplementary Table 8). Interestingly, the results indicated this syntenic block was retained from a whole genome duplication event taken place during the time span of the zygomorphic flower emergences (about 60 million years ago). Furthermore, downstream *CYC/DICH*, two genes (*DIV* and *DRIF*) in *RAD*/*DIV* module have homologous copies with similar Ks as *CYC*/*DICH*, while *DRIF* is located at a WGD derived syntenic block[19,20,21]. Those analyses showed that the master regulators of zygomorphic flower were retained from the recent whole genome duplication, revealing the evolutionary base for the zygomorphic flower maintenance in *A. majus* and perhaps other close relatives.

To further explore TCP family evolution among other zygomorphic flower species, we extended the syntenic block and *Ks* analyses to *M. truncatula*, belonging to legume[22]. The results showed that *M. truncatula* independently undergone a recent whole genome duplication event around the similar time as *A. majus* without similar duplicated *CYC*/*DICH* copies, suggesting that *A. majus* harbored a unique genetic mechanism for zygomorphic flower (Supplementary Figure 8). Though we could not couple the genetic events with the appearance of zygomorphic flower, our TCP family analysis on representative angiosperms indicated that the genetic origins of zygomorphic flower were ancient and occurred around the late period of Cretaceous about 60 MYA (Figure 3).

Previous phylogenetic analysis suggested that zygomorphic flower independently evolved from actinomorphic ancestors for more than 25 times[23].Our

212 findings indicated that gene duplications are involved in a genetic robustness of
213 zygomorphic flower evolution by maintaining copies of master regulators.

214 **Structure of the *ψS*-locus in *A. majus* and its gene collinearity in SI species**

215 Previously, we found the *Antirrhinum S*-locus is located in a heterochromatin region
216 on the short arm of chromosome 8 through cytological investigation[24]. To reveal a
217 complete pseudo (*ψ*)*S*-locus in self-compatible *A. majus*, we scan conserved regions
218 (FBA/FBK domain) of *SLF* gene family in the assembled *A. majus* genome, we
219 identified the *S* genes located in the short arm of chromosome 8 and examined their
220 expressions inside the *ψS*-locus region. The locus consists of 37 *SLF* genes
221 (*SLF1-SLF37*) covering 874 kb composed of three scaffolds *Sc29, Sc276* and *Sc184*
222 (Figure 4a). Six pseudogenes with FBA domains were inferred to be loss-of-function
223 in evolution. No S-RNase was found in and near the region, suggesting it might be
224 lost in self-compatible *A. majus*. *RAD* gene locates in the upstream of *SLF1* gene
225 about 1Mb, consistent with previous studies showing its linkage with the *S*-locus[24];
226 and the region contains 102 genes from *RAD* to *SLF37*. Most *SLF* genes are expressed
227 in pollen or anther indicating they could be related to pollination and fertilization.
228 Taken together, these results showed that we obtained a near complete *ψS*-locus with
229 the largest numbers of *S* genes annotated in a plant genome (Figure 4b and
230 Supplementary Excel 4-6).

231 To explore the *S*-locus structures between SC and SI species, we compared the
232 *ψS*-locus sequence with nine assembled TAC (Transformation-competent artificial
233 chromosome) sequences from four *S* haplotypes of self-incompatible *A. hispancum*
234 and uncovered high gene collinearity between *AhSLF12* and *AhSLF13* except for
235 *AhSLF32* located in S_2, S_4 and S_5 haplotypes of *A. hispanicum* (Figure 4c). An
236 intra-chromosome inversion around the *S*-locus occurred in the S_2 haplotype of *A.*
237 *hispanicum* as described previously. However, no apparent large collinearity was
238 found between *A. majus* and TAC sequences containing the *S-RNase* gene, supporting

239 that the region containing *S-RNase* was deleted in the *ψS*-locus. We found one
240 orthologous pseudo-gene in *A. majus*, *AmSLF18* on chromosome 8, which has a
241 complete corresponding coding sequence region and expressed in the S_4 haplotype,
242 suggesing a recent duplication event (Figure 4c, Supplementary Excel 7).
243 To examine the evolution of *SLF and S-RNase* genes, the *Ka* and *Ks* rate of the
244 twelve collinear *SLF* gene pairs showed that the values of *SLFs* are lower than that of
245 *S-RNase* in *Antirrhinum*, and the allelic *SLF* genes showed a Ka/Ks=0.41, consistent
246 with a negative frequency-dependent selection detected previously. Only *SLF14*
247 appears to be a positively selected gene (Ka/Ks>1) (Supplementary Excel 8). The
248 average divergence time of these *SLF* orthologous genes was estimated to be 4
249 million years ago consistent with the early *Antirrhinum* species divergence of less
250 than 5.3 million years. The average divergence time of these *S-RNases* is estimated to
251 be around 90 MYA, consisting with the species divergence between *Antirrhinum* and
252 Solanaceae species (Supplementary Excel 9).
253 Taken together, our results showed that the *Antirrhinum S*-locus is shaped by
254 allelic synteny, purifying selection, gene conversion, transposition and
255 pseudogenization .
256
257 **Discussion**
258 In this study, we have successfully obtained a chromosome-scale fine genome of *A.*
259 *majus*, representing the first sequenced genome in Plantaginaceae. This genome
260 provides a useful resource for evolutionary and molecular studies on key genes
261 controlling complex traits in the classical eudicot model species. The comparison of
262 404 gene families' expansions and 191 contractions in *A. majus* genome with those of
263 nine other fully sequenced diverse plant species showed several specific evolutionary
264 paths of important gene families, such as those involved in metabolism and signaling
265 pathways. Furthermore, the absence of a recent WGT in *Antirrhinum* genome makes it
266 a key diploid genome that promises to provide important insights into plant genome

evolution. Recently, small RNAs in natural hybrid zone of *A. majus* using this genome sequence as a reference have revealed an inverted duplication acting as steep clines by nature selection in evolution of flower color pattern[25].

Complex traits, such as zygomorphic type flower in *Antirrhinum*, often couple with different gene duplication events. The zygomorphic structure in *Antirrhinum* occurred in late period of Cretaceous, consistent with its role in facilitating insect-mediated pollination. We demonstrated that the morphology of floral organ was associated with several gene duplication events and revealed the divergence of *A. majus* from other angiosperms. Although *Antirrhinum* did not experience a whole genome triplication, the duplicated region containing TCP genes on chromosomes 6 and 8 are closely associated with zygomorphic flower type, showing its unique evolutionary manner because no similar mechanism had been found in closely related species. For examples, one separated whole genome duplication led to partial zygomorphic type species of Glycine; and a MADS box family gene change resulting in symmetrical flowers in Orchidaceae[26,27]. In general, the ancient species are mostly radial symmetry and the newly derived species with symmetrical flowers. Studies on *Antirrhinum* floral mutants supported that these two copies play a role in controlling symmetrical flower, which makes the petals polar, and the flower structure tends to be upright and is beneficial to the use of light and attracting pollinators. This mechanism could be further verified by genetic analysis in a relative species.

SI also is a complex trait controlled by the *S*-locus[2,3]. The fine genomic structure of the *ψS*-locus from *A. majus* showed that the large number of pollen *SLFs* could be a result of recombination suppression, gene duplication, purifying selection and frequency-dependent selection[28]. These evolutionary processes could be the intrinsic mechanisms to maintain the low allelic diversity of orthologous *SLFs* because extensive divergence would lead to self-inactivation of S-RNase resulting in loss of SI. The deletion of S-RNase in cultivated *A. majus* could be directly associated with the loss of SI, resulting in an irreversible evolutionary process, because loss of

295 self-incompatibility of SI species often results in compatible ones and SC species are
296 difficult or almost impossible to reverse back to self-incompatible species (Doll's
297 Law) [29]. The high microcollinearity of the *S*-locus between SI and SC of *Antirrhinum*
298 indicated that the deletion of *S-RNase* in SC species was a recent event. Some
299 mutated *SLF* genes in different haplotypes were also evolved recently. Loss of
300 *S-RNase* at the *S*-locus would have little consequence for the pollen phenotype while
301 duplications would lead to expression of two types of *SLFs* which could inactivate a
302 broader range of incoming S-RNases. Further genome analysis of additional SI
303 species of *Antirrhinum* should provide an insight into its evolutionary status.
304 Intriguingly, the physical size of the *S*-locus in *S. lycopersicum* (17 Mb,
305 containing 17 *SLF* genes) is much larger than that in *A. majus* (2 Mb, containing 37
306 *SLF* genes) [30]. This appears to indicate that increasing the gene numbers through
307 in-locus unequal crossovers and repetitive element enrichments by a hitchhike effect
308 could result in its large physical size and low gene density of the *S*-locus in tomato.
309 Rich retrotransposons and unique small regulatory RNAs associated with the *S*-loci of
310 *Solanum* and *Antirrhinum*, respectively, appear to indicate the differential epigenetic
311 modifications could contribute to the locus density puzzle between these species.
312 In conclusion, the high-quality genome sequence obtained in this work could be
313 used as a reference genome for Plantaginaceae and will be helpful for genetic,
314 genomic and evolutionary studies in both *Antirrhinum* and other flowering plants.
315

URLs

Genome assembly data has been deposited at NCBI BioProject ID under accession codes PRJNA227267 and Biosample ID under accession codes SAMN02991092. We built the website of *Antirrhinum* genome http://bioinfo.sibs.ac.cn/Am.

Methods

Methods and any associated references are available in the online version of the paper.

Acknowledgements

This work was supported by the Ministry of Science and Technology of China (2013CB945102) and the National Natural Science Foundation of China (31401045 and 31221063). We thank Zhixi Tian for help of CACTA transposon analyses.

Author contributions

Y.X., H.Z., D.Z. and M.L. designed the experiments; M.L., D.Z. and Y.X. wrote the manuscript. Q.G, B.M., C.C., Y.L., Q.L., Y.Z., H.G., J.L., Y.Z., Y.S., L.C., A.W., Y.C., Y.L., M.Q., J.W., Y.C., D.W., J.Z., G.L., B.W., L.Y., C.X., J.L., S.Z., Y.Z, S.H., C.L., Y.Y., E.C. and Y.X. analyzed the data and performed the experiments.

References

1 Schwarz-Sommer, Z., Davies, B. & Hudson, A. An everlasting pioneer: the story of *Antirrhinum* research. *Nat Rev Genet* **4**, 655-664, doi:10.1038/nrg1127 (2003).

2 Nettancourt, D. Incompatibility in angiosperms. (*Springer-Verlag Berlin Heidelberg New York*) (1977).

3 Franklin-Tong, V. E. Self-incompatibility in flowering plants. (*Springer*) (2008).

4 Coen, E. S., Carpenter, R. & Martin, C. Transposable elements generate novel spatial patterns of gene expression in *Antirrhinum majus*. *Cell* **47**, 285-296 (1986).

5 Sommer, H., Beltrán, J.P. &Huijser, P. Deficiens, a homeotic gene involved in the control of flower morphogenesis in *Antirrhinum majus*: the protein shows homology to transcription factors. *EMBO J.* **9**, 605-13 (1990).

6 Tröbner, W., Ramirez, L. & Motte, P. *GLOBOSA*: a homeotic gene which interacts with *DEFICIENS* in the control of *Antirrhinum* floral organogenesis. *EMBO J.* 11 4693–4704 (1992).

7 Luo, D., Carpenter, R., Vincent, C., Copsey, L. & Coen, E. Origin of floral asymmetry in *Antirrhinum*. *Nature* **383**, 794-799 (1996).

8 Luo, D., Carpenter, R., Copsey, L., Vincent. C, Clark. J, & Coen, E. Control of Organ Asymmetry in Flowers of *Antirrhinum*. *Cell* **99**, 367-376 (1999).

9 Glover, B. J., Perez-Rodrigues, M. & Martin, C. Development of several epidermal cell types can be specified by the same MYB-related plant transcription factor. *Development* **125**, 3497-3508 (1998)

10 Schwinn, K., Venail, J., Shang, Y., Mackay, S., Alm, V., Butelli, E., Oyama, R., Bailey, P., Davies, K. & Martin, C. A small family of MYB□regulatory genes controls floral pigmentation intensity and patterning in the genus *Antirrhinum*. *Plant Cell* **18**, 831–851 (2006).

11 Lai, Z. *et al.* An F-box gene linked to the self-incompatibility (S) locus of *Antirrhinum* is expressed specifically in pollen and tapetum. *Plant Mol Biol* **50**, 29-42 (2002).

12 Lee, H. S., Huang, S. & Kao, T. S proteins control rejection of incompatible pollen in Petunia inflata. *Nature* **367**, 560-563, doi:10.1038/367560a0 (1994).

13 Qiao, H. *et al.* The F-box protein AhSLF-S2 controls the pollen function of S-RNase-based self-incompatibility. *Plant Cell* **16**, 2307-2322, doi:10.1105/tpc.104.024919 (2004).

14 Hudson, A., Critchley, J. & Erasmus, Y. The genus *Antirrhinum* (snapdragon): a flowering plant model for evolution and development. *CSH Protoc.* doi: 10.1101/pdb.emo100 (2008).

15 Corley, S.B., Carpenter, R., Copsey, L. &Coen, E. Floral asymmetry involves an interplay between TCP and MYB transcription factors in *Antirrhinum*. *Proc Natl Acad Sci U S A.* **102**(14):5068-73 (2005).

16 Sonah, H., Bastien, M., Iquira, E., Tardivel, A., Le ´gare ´, G., Boyle, B., Normandeau, E., Laroche, J., Larose, S., Jean, M., et al. An improved genotyping by sequencing (GBS) approach offering increased versatility and efficiency of SNP discovery and genotyping. PLoS One **8**: e54603 (2013).

17 Bowers, J. E., Chapman, B. A., Rong, J. & Paterson, A. H. Unravelling angiosperm genome evolution by phylogenetic analysis of chromosomal duplication events. *Nature* **422**, 433-438, doi:10.1038/nature01521 (2003).

18 Cubas P., Lauter N., Doebley J. & Coen E. The TCP domain: a motif found in proteins regulating plant growth and development. *Plant J.* **18**, 215–222 (1999).

19 Preston, J.C., Martinez, C.C.&Hileman, L.C. Gradual disintegration of the floral symmetry gene network is implicated in the evolution of a wind-pollination syndrome. Proc Natl Acad Sci U S A. **108** (6):2343-8 (2011)

20 Raimundo, J., Sobral, R., Bailey, P., Azevedo, H., Galego, L., Almeida, J., Coen, E.&Costa MM. A subcellular tug of war involving three MYB-like proteins underlies a molecular antagonism in *Antirrhinum* flower asymmetry. *Plant J.* **75** (4):527-38 (2013).

21 Reardon, W., Gallagher, P., Nolan, K.M., Wright, H., Cardeñosa-Rubio, M.C., Bragalini, C., Lee, C.S., Fitzpatrick, D.A., Corcoran, K., Wolff, K., Nugent, J,M. Different outcomes for the MYB floral symmetry genes DIVARICATA and RADIALIS during the evolution of derived actinomorphy in Plantago. New Phytol. **202**(2):716-25 (2014).

22 Young, N.D. et al., The Medicago genome provides insight into the evolution of rhizobial symbioses. *Nature* **480** (7378):520-4 (2011).

23 Donoghue, M., Ree, R.&Baum, D. Phylogeny and the evolution of flower symmetry in the Asteridae. *Trends in Plant Science* **3**:311–317 (1998).

24 Yang, Q., Zhang, D., Li, Q., Cheng, Z. & Xue, Y. Heterochromatic and genetic features are consistent with recombination suppression of the self-incompatibility locus in *Antirrhinum*. *Plant J* **51**, 140-151 (2007).

25 Bradley, D., Xu, P., Mohorianu, II., Whibley, A., Field, D., Tavares, H., Couchman, M., Copsey, L., Carpenter, R., Li, M., Li, Q., Xue, Y., Dalmay, T.& Coen, E. Evolution of flower color pattern through selection on regulatory small RNAs. *Science* **358** (6365):925-928 (2017).

26 Feng, X., Zhao, Z., Tian, Z., Xu, S., Luo, Y., Cai, Z., Wang, Y., Yang, J., Wang, Z., Weng, L., Chen, J., Zheng, L., Guo, X., Luo, J., Sato, S., Tabata, S., Ma, W., Cao, X., Hu, X.&Sun C, Luo D. Control of petal shape and floral zygomorphy in Lotus japonicus. *Proc Natl Acad Sci U S A.* **103** (13):4970-5 (2006).

27 Zhang et.al The Apostasia genome and the evolution of orchids. *Nature* 2017 **549**(7672):379-383 (2017).

411 28 Wright, S. The distribution of self-sterility alleles in populations. *Genetics* **24**,
412 538-552 (1939).

413 29 Igic, B., and Kohn, J.R. The distribution of plant mating systems: study bias
414 against obligately outcrossing species. *Evolution* **60**, 1098-1103 (2006).

415 30 Li, W. & Chetelat, R. T. Unilateral incompatibility gene ui1.1 encodes an
416 S-locus F-box protein expressed in pollen of Solanum species. *Proc Natl Acad*
417 *Sci U S A* **112**, 4417-4422 (2015).

418

Figures

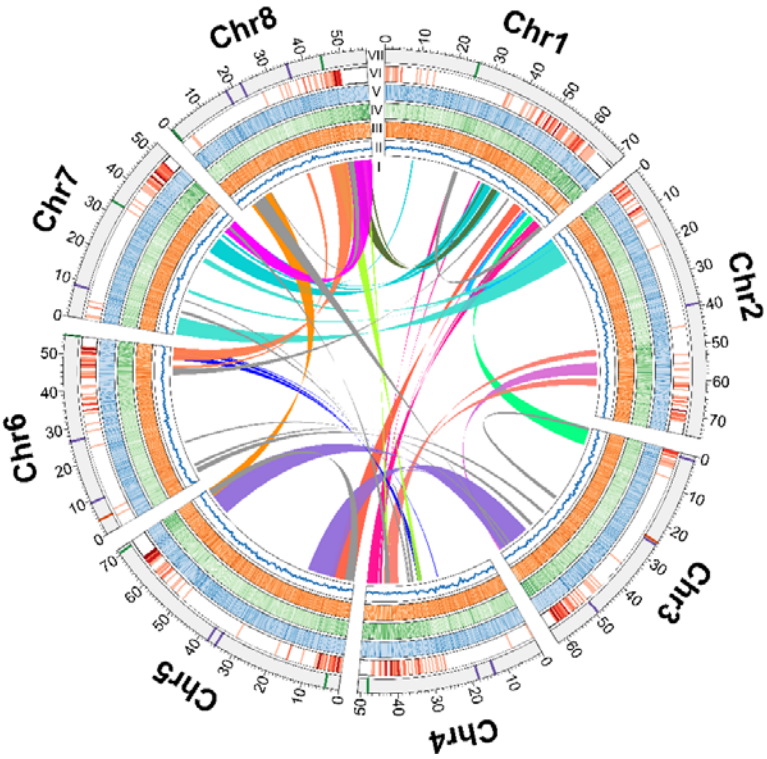

Figure 1. Genomic structure overview of *Antirrhinum majus* JI7.

(I) Duplications of genomic paralogous sequences; (II) GC content.In II, III, IV, and V, deep colors show high density genes or repeat sequence regions; (III) Simple sequence repeats; (IV) Gene density; (V) Retroelement density; (VI) Recombination rate. Deep color shows high recombination rates.); (VII) Eight Antirrhinum chromosomes with physical distances including low copy number repetitive elements: telomere repeat TTTAGGG (green), 5S rDNA (orange), pericentromeric repeats CentA1 and CentA2 (purple).

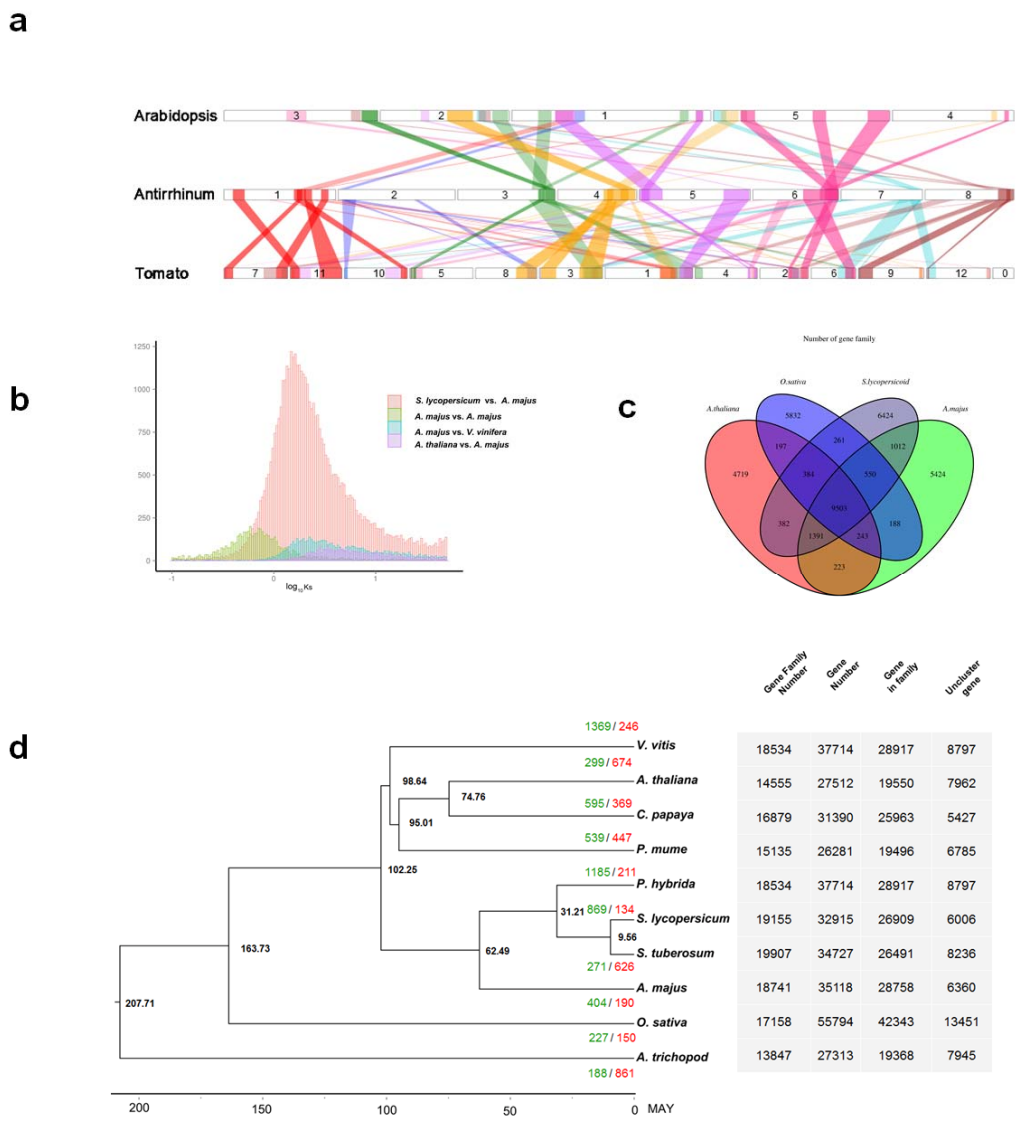

Figure 2. Genome evolution of *A. majus*.

a Synteny blocks among chromosomes of *A. majus*, *S. lycopersicum* and *A. thaliana*. The numbers represent individual chromosomes. The selected syntenic gene number more than fifty.

b Density distributions of Ks for paralogous genes.

c A Venn diagram of shared orthologues among four species. Each number represents a gene family number. Venn diagram of annotated gene families showing shared

orthologous groups among the genomes of *A. majus*, *S. lycopersicum*, *A. thaliana*, and *O. sativa*.

d Phylogenetic tree of 10 angiosperm species including their divergence time based on orthologues of single-gene families. The number in each node indicates the number of gene families. *A. trichopoda* used as an outgroup. Bootstrap values for each node are above 100%.

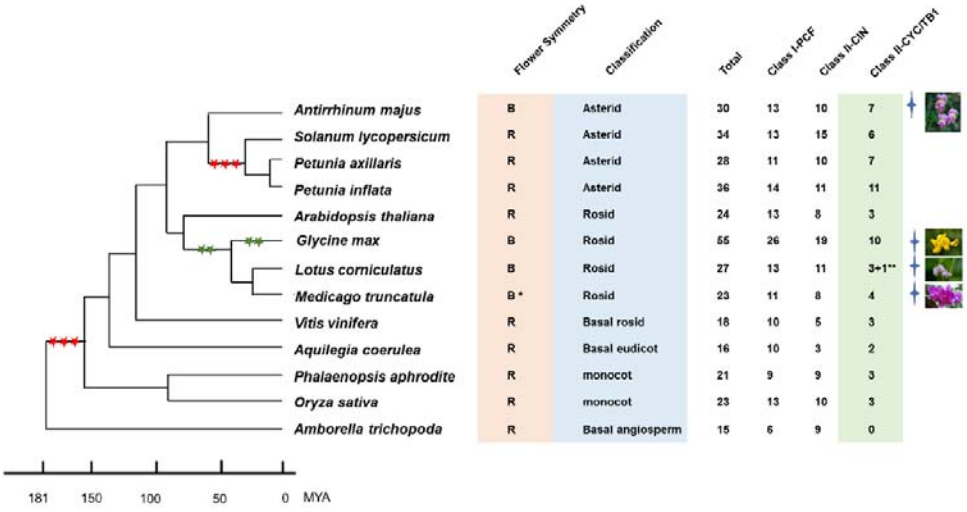

Figure 3. Evolution of flower symmetry and TCP gene family.

Left shows a phylogenetic tree of the flowering plants derived from their divergence time based on orthologues of single-gene families. Three red stars show the whole genome triplication and two green stars the duplication events. “B” represents bilateral flower symmetry and “R” radial flower symmetry; Asterid, Rosid, Basal rosid, Basal eudicot, Monocot and Basal angiosperm represent their clades, respectively. Total numbers of TCP family genes, Class I-PCF, Class II-CIN and Class II-CYC/TB1 are shown from left to right. * indicates the sequenced genome of species of *Medicago truncatula* with flower radial symmetry, but flowers of most *Medicago* species are of bilateral symmetry. ** indicates *Lotus comiculatus* in which three TCP genes were identified but a functional TCP gene was not detected in its genome. Four-pointed stars denote bilateral symmetry flowers with their photos from PPBC (http://www.plantphoto.cn).

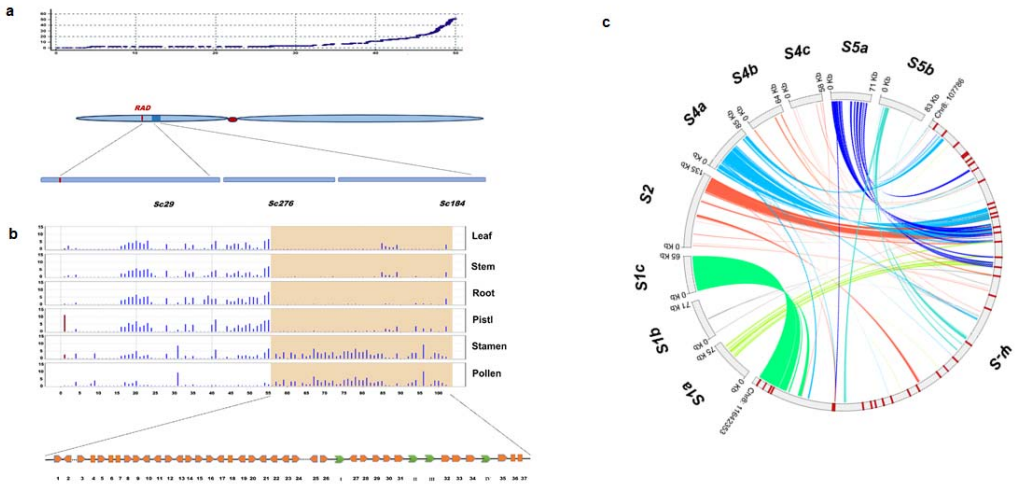

Figure 4. Genomic features of the *ψS*-locus of *A. majus* and its synteny with the *S*-locus regions of *A. hispanicum*.

a Chromosomal locations of three scaffolds covering the *ψS*-locus region of *A. majus*. A genetic recombination map of chromosome 8 is shown on the top panel. The x-axis shows its physical distance and the y-axis its genetic distance. A schematic representation of chromosome 8 is shown in the middle panel with a red dot indicating its centromere. The *ψS*-locus is depicted as a blue box on its short arm. A vertical red line in chromosome indicates *RAD* gene. The low panel shows three scaffolds of *Sc29*, *Sc276*, and *Sc184* covering the *ψS*-locus region.

b Transcriptional profiles of the *ψS*-locus and its flanking regions of *A. majus*. The light yellow shadow denotes the predicted *ψS*-locus region (*SLF1-SLF37*). This region between *RAD* and *SLF37* contains a total number of 102 annotated genes. The bottom part is a schematic representation of the *SLF* genes. Orange squares indicate the *ψSLF* genes and green arrows the other annotated genes (I: a putative MYB family transcription factor; II and III, putative RNA-binding proteins; and IV, a putative phosphate-dependent transferase)

c The synteny of the *S*-locus regions between *A. majus* and S_1, S_2, S_4 and S_5 haplotypes of *A. hispanicum*. Different colors indicate syntenic and inversion regions between the ψS-locus and S_1 (S_{1a}, S_{1b} and S_{1c}), S_2, S_4 (S_{4a}, S_{4b} and S_{4c}) or S_5(S_{5a} and S_{5b}) haplotypes of *A. hispanicum*.

Table 1 Statistics for the Antirrhinum genome and gene annotation

Estimate of genome size	520 Mb
GC content	35.50%
N50 length (contig)	0.73 Mb
Longest contig	3.74 Mb
Total size of assembled contigs	510.00 Mb
N50 length (scaffold)	2.62 Mb
Longest scaffold	9.90 Mb
Total size of assembled scaffolds	511.70 Mb
Number of genes	37714
Average gene length	3166 bp
Gene density	73.95 Mb^{-1}
Transcripts number	52780
Average CDS length	1036 bp
Average protein length	344 aa
Average exon length	245 bp
Average intron length	314 bp
Tandem repeat	13.03 Mb

480

Figures

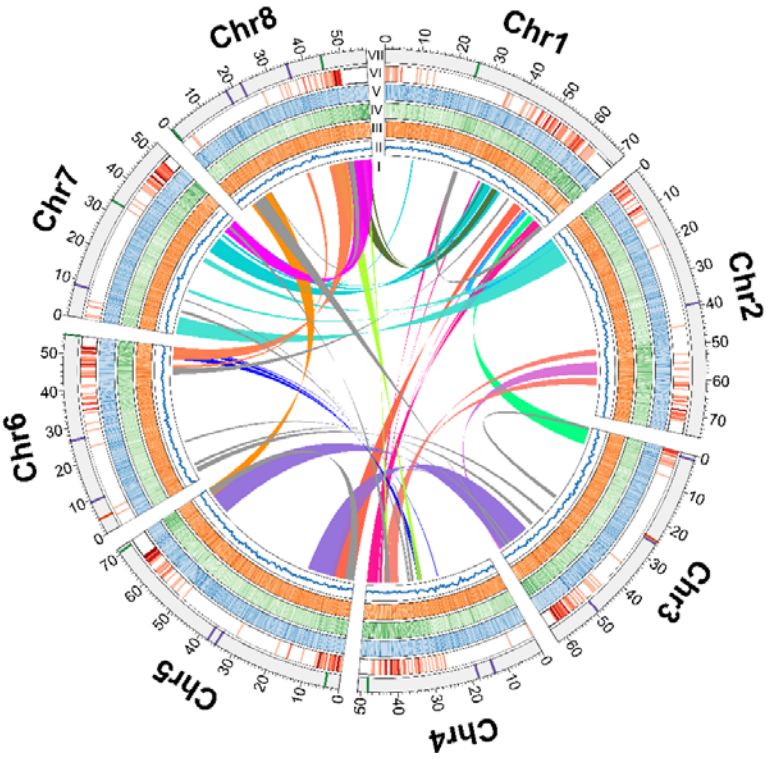

Figure 1. Genomic structure overview of *Antirrhinum majus* JI7.

(I) Duplications of genomic paralogous sequences; (II) GC content.In II, III, IV, and V, deep colors show high density genes or repeat sequence regions; (III) Simple sequence repeats; (IV) Gene density; (V) Retroelement density; (VI) Recombination rate. Deep color shows high recombination rates.); (VII) Eight Antirrhinum chromosomes with physical distances including low copy number repetitive elements: telomere repeat TTTAGGG (green), 5S rDNA (orange), pericentromeric repeats CentA1 and CentA2 (purple).

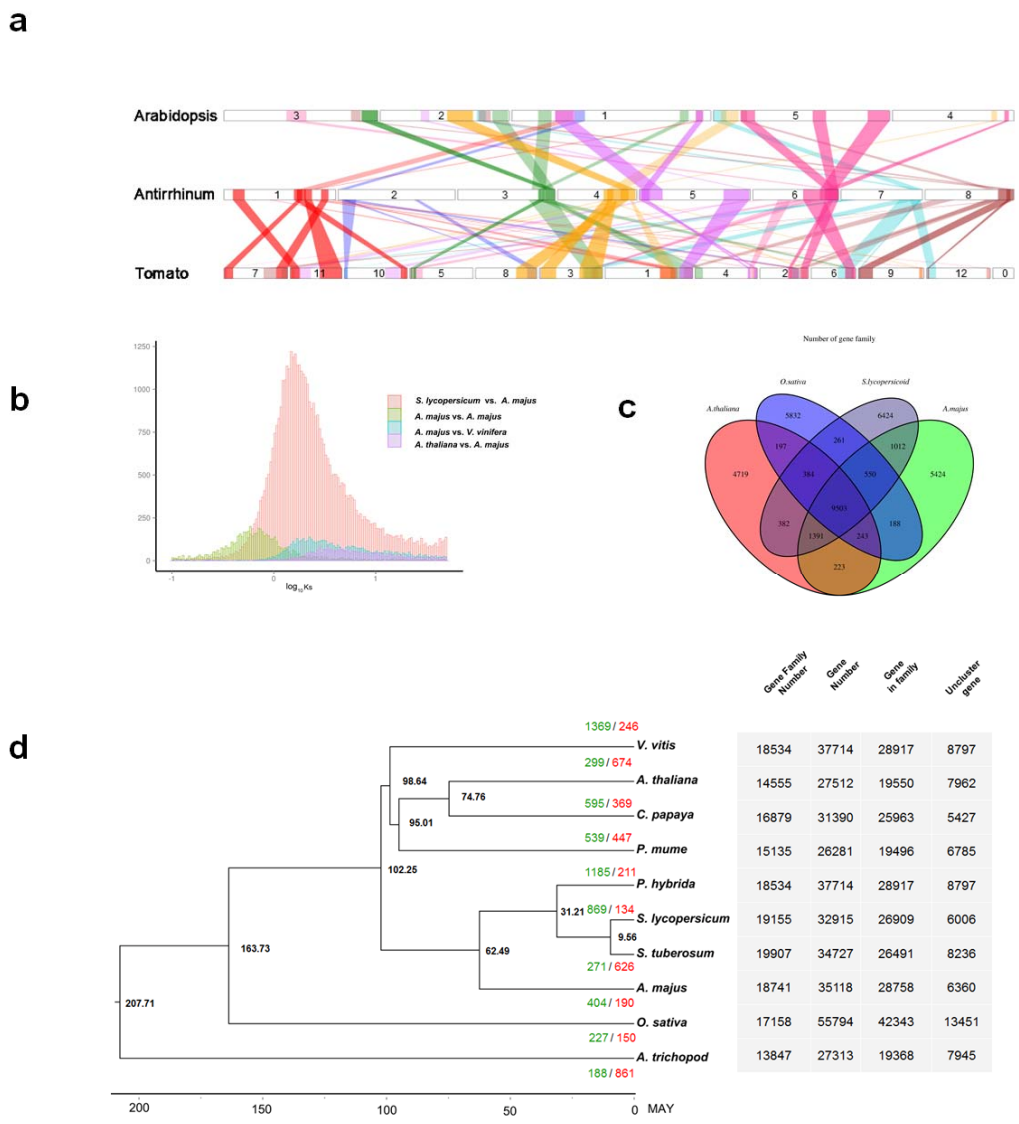

Figure 2. Genome evolution of *A. majus*.

a Synteny blocks among chromosomes of *A. majus*, *S. lycopersicum* and *A. thaliana*. The numbers represent individual chromosomes. The selected syntenic gene number more than fifty.

b Density distributions of Ks for paralogous genes.

c A Venn diagram of shared orthologues among four species. Each number represents a gene family number. Venn diagram of annotated gene families showing shared orthologous groups among the genomes of *A. majus*, *S. lycopersicum*, *A. thaliana*, and *O. sativa*.

d Phylogenetic tree of 10 angiosperm species including their divergence time based

on orthologues of single-gene families. The number in each node indicates the number of gene families. *A. trichopoda* used as an outgroup. Bootstrap values for each node are above 100%.

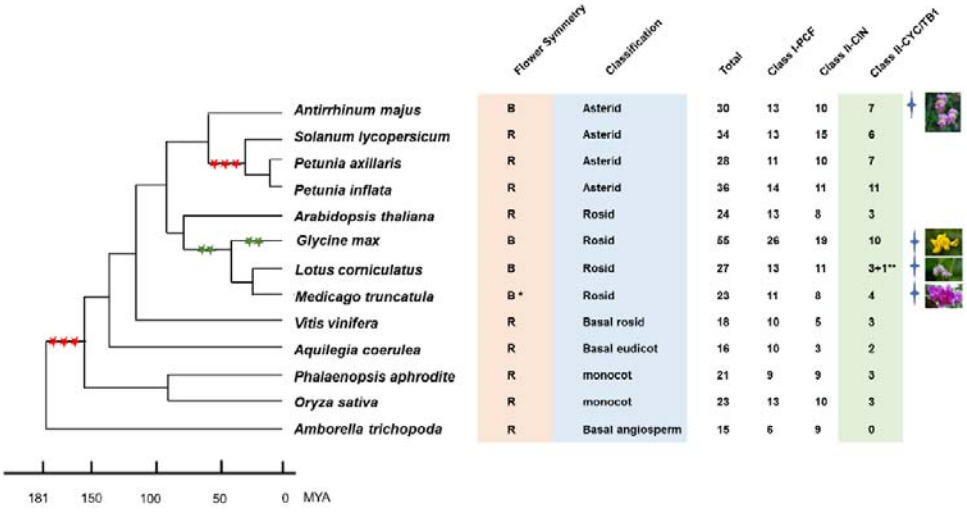

Figure 3. Evolution of flower symmetry and TCP gene family.

Left shows a phylogenetic tree of the flowering plants derived from their divergence time based on orthologues of single-gene families. Three red stars show the whole genome triplication and two green stars the duplication events. “B” represents bilateral flower symmetry and “R” radial flower symmetry; Asterid, Rosid, Basal rosid, Basal eudicot, Monocot and Basal angiosperm represent their clades, respectively. Total numbers of TCP family genes, Class I-PCF, Class II-CIN and Class II-CYC/TB1 are shown from left to right. * indicates the sequenced genome of species of *Medicago truncatula* with flower radial symmetry, but flowers of most *Medicago* species are of bilateral symmetry. ** indicates *Lotus comiculatus* in which three TCP genes were identified but a functional TCP gene was not detected in its genome. Four-pointed stars denote bilateral symmetry flowers with their photos from PPBC (http://www.plantphoto.cn).

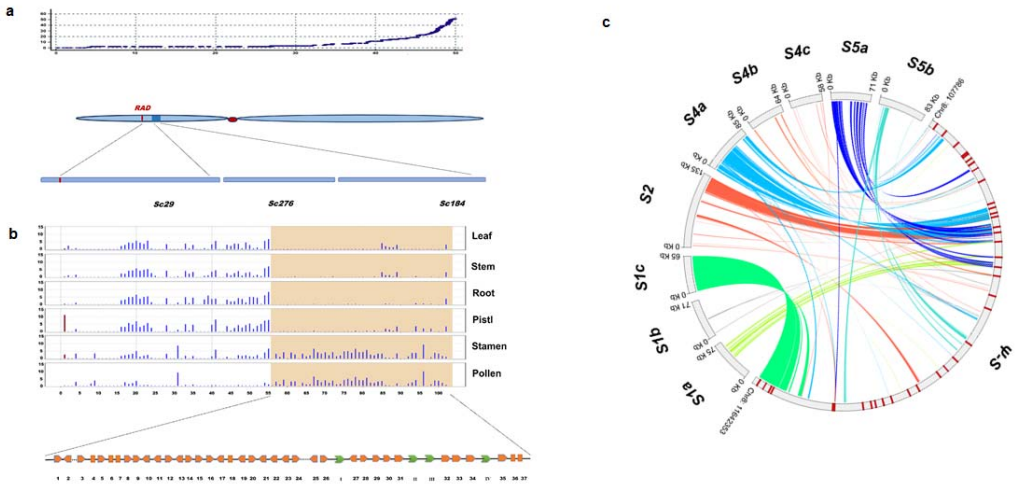

Figure 4. Genomic features of the *ψS*-locus of *A. majus* and its synteny with the *S*-locus regions of *A. hispanicum*.

a Chromosomal locations of three scaffolds covering the *ψS*-locus region of *A. majus*. A genetic recombination map of chromosome 8 is shown on the top panel. The x-axis shows its physical distance and the y-axis its genetic distance. A schematic representation of chromosome 8 is shown in the middle panel with a red dot indicating its centromere. The *ψS*-locus is depicted as a blue box on its short arm. A vertical red line in chromosome indicates *RAD* gene. The low panel shows three scaffolds of *Sc29*, *Sc276*, and *Sc184* covering the *ψS*-locus region.

b Transcriptional profiles of the *ψS*-locus and its flanking regions of *A. majus*. The light yellow shadow denotes the predicted *ψS*-locus region (*SLF1-SLF37*). This region between *RAD* and *SLF37* contains a total number of 102 annotated genes. The bottom part is a schematic representation of the *SLF* genes. Orange squares indicate the *ψSLF* genes and green arrows the other annotated genes (I: a putative MYB family transcription factor; II and III, putative RNA-binding proteins; and IV, a putative phosphate-dependent transferase)

c The synteny of the *S*-locus regions between *A. majus* and S_1, S_2, S_4 and S_5 haplotypes of *A. hispanicum*. Different colors indicate syntenic and inversion regions

between the *ψS*-locus and S_1 (S_{1a}, S_{1b} and S_{1c}), S_2, S_4 (S_{4a}, S_{4b} and S_{4c}) or S_5(S_{5a} and S_{5b}) haplotypes of *A. hispanicum*.